

DYNAMO ACTION IN THE SOLAR CONVECTION ZONE AND TACHOCLINE: PUMPING AND ORGANIZATION OF TOROIDAL FIELDS

MATTHEW K. BROWNING¹, MARK S. MIESCH², ALLAN SACHA BRUN³, AND JURI TOOMRE⁴

¹ Astronomy Department, University of California at Berkeley, 601 Campbell Hall, Berkeley CA 94720-3411, matthew@astro.berkeley.edu,

²High Altitude Observatory, NCAR, Boulder, CO 80307-3000,

³DSM/DAPNIA/SAP, CEA Saclay, 91191 Gif sur Yvette, France,

⁴JILA and Department of Astrophysical and Planetary Sciences, University of Colorado, Boulder, CO 80309-0440

Received 16 Jun 2006; Accepted 24 Jul 2006; In press

ABSTRACT

We present the first results from three-dimensional spherical shell simulations of magnetic dynamo action realized by turbulent convection penetrating downward into a tachocline of rotational shear. This permits us to assess several dynamical elements believed to be crucial to the operation of the solar global dynamo, variously involving differential rotation resulting from convection, magnetic pumping, and amplification of fields by stretching within the tachocline. The simulations reveal that strong axisymmetric toroidal magnetic fields (about 3000 G in strength) are realized within the lower stable layer, unlike in the convection zone where fluctuating fields are predominant. The toroidal fields in the stable layer possess a striking persistent antisymmetric parity, with fields in the northern hemisphere largely of opposite polarity to those in the southern hemisphere. The associated mean poloidal magnetic fields there have a clear dipolar geometry, but we have not yet observed any distinctive reversals or latitudinal propagation. The presence of these deep magnetic fields appears to stabilize the sense of mean fields produced by vigorous dynamo action in the bulk of the convection zone.

Subject headings: convection – MHD – Sun: magnetic fields – turbulence

1. ELEMENTS OF SOLAR DYNAMO

The solar global dynamo responsible for the observed 22-year cycles of magnetic activity is likely to require several dynamical processes operating at differing sites within the convection zone and below its base. The primary elements were first discussed within the conceptual “interface dynamo” proposed by Parker (1993) and then explored by Charbonneau & MacGregor (1997). The key dynamical processes involve (a) the generation of magnetic fields by the intense turbulence influenced by rotation within the deep solar convection zone, (b) the transport or pumping of these fields downward into the tachocline of shear at the base of this zone, (c) the stretching of fields there by differential rotation to form strong toroidal fields, and (d) the magnetic buoyancy instability of such structures leading to field loops ascending toward the surface. Fully self-consistent magnetohydrodynamic (MHD) simulations of the complete solar global dynamo are not yet feasible, given the vast range of dynamical scales involved in these turbulent processes. However, many of the elements have now begun to be studied singly with reasonable fidelity using three-dimensional numerical modelling, often turning to localized planar domains to obtain sufficient spatial resolution within the simulations (see reviews by Ossendrijver 2003, Fan 2004, Charbonneau 2005, Miesch 2005).

Yet some aspects require using full spherical shell geometries in the modelling. Early simulations of dynamo processes in spherical shells provided insights into the coupling of convection, rotation and magnetism, but were limited by spatial resolution (e.g., Gilman 1983; Glatzmaier 1985a, b). Recent studies of the interaction of turbulent convection with rotation (e.g., Miesch et al. 2000; Brun & Toomre 2002; Miesch, Brun & Toomre 2006) now yield global differential rotation profiles in close accord with helioseismic deductions (e.g., Thompson et al. 2003) in the bulk of the convection zone. Similarly, related MHD modelling of dynamo processes

in such deep shells of turbulent convection has revealed that strong magnetic fields are produced without diminishing the differential rotation significantly (Brun, Miesch & Toomre 2004, hereafter BMT04). Fluctuating magnetic fields with strengths of order 5000 G are realized that possess complex structures, with radial fields concentrated in downflow lanes and toroidal fields appearing as twisted ribbons extended in longitude. However, the associated mean fields are relatively weak and do not exhibit the systematic latitudinal propagation or periodic polarity reversals seen in the Sun. Whereas BMT04 only considered dynamical element (a), we report here on also incorporating elements (b) and (c) into global simulations of dynamo action achieved by turbulent convection able to penetrate downward into a tachocline of rotational shear. Such modeling is the next step in refining our intuition about the operation of the interface dynamo.

2. CONVECTIVE SHELL WITH PENETRATION AND FORCED TACHOCLINE

We conduct three-dimensional nonlinear MHD simulations of convection and dynamo action in a rotating spherical shell using the anelastic spherical harmonic pseudospectral code ASH (see Clune et al. 1999 and BMT04). ASH is based upon a large-eddy simulation (LES) approach involving subgrid-scale (SGS) modelling of unresolved turbulent processes. Our studies here extend the modelling of BMT04 by allowing penetration of the convection downward into a region of stable stratification, where the pronounced differential rotation maintained by the convection is forced to vanish, thereby establishing a tachocline of shear. Our computational domain extends over 0.62–0.96 R , where R is the solar radius, spanning the bulk of the solar convection zone and part of the radiative interior below. Solar values are used for the rotation rate and luminosity, and the initial stratification is obtained from a one-dimensional solar structure model. We adopt a softer subadiabatic stratification in the lower stable zone to

ease our numerical resolution of internal gravity waves produced by the overshooting motions (see Miesch et al. 2000).

The tachocline as revealed by helioseismology is a narrow transition boundary layer between the differentially rotating convection zone (fast equator, slow poles) and the uniformly rotating radiative interior. Its discovery motivated the interface dynamo paradigm. The detailed structure of the tachocline may be determined variously by anisotropic turbulent mixing processes, magnetic stresses, and production of internal gravity waves; the equilibration times likewise continue to engender debate (see review by Miesch 2005). Despite uncertainties, a tachocline of rotational shear is crucial to element (c), and thus we seek to impose one here in two complementary ways. First, we introduce a drag force upon the axisymmetric velocities (relative to our rotational frame) to force them to vanish at the base of the computational domain. We accomplish this smoothly with a hyperbolic tangent (of width $0.01 R$ centered at $0.66 R$ in the stable layer) so that motions within the bulk of the convective envelope are unimpeded. Without this forcing, the differential rotation established self-consistently within the convection zone would imprint itself upon the radiative zone through viscous and thermal diffusion. Second, we impose within the overshooting region a weak latitudinal entropy variation to emulate the coupling between the convective envelope and the radiative interior through thermal wind balance within the solar tachocline. This is achieved by thermal forcing, involving a monotonic increase in temperature of about 6 K from equator to pole at the base of convection zone (over a width of $0.02 R$), much as discussed by Miesch, Brun & Toomre (2006, hereafter MBT06). The thermal forcing aids in achieving a strong latitudinal differential rotation within the convection zone, which otherwise would be diminished by coupling to the radiative interior. This coupling is much stronger in our simulations than in the Sun because the viscous and thermal diffusivities are far larger and the overshoot region is wider.

The domain boundaries are assumed to be impenetrable and free of viscous stresses. The lower boundary is assumed to be a perfect conductor and the radial entropy gradient is fixed there. At the upper boundary the magnetic field within the domain is matched to an external potential field and the entropy is fixed. The simulations were initiated by adding a weak seed field to a progenitor penetrative hydrodynamic simulation. The seed field was toroidal and confined to the bulk of the convection zone. For the present model, we employ a horizontal resolution of $N_\theta = 512$, $N_\phi = 1024$, and a stacked Chebyshev expansion in the radial dimension with $N_r = 98$. The effective SGS viscosity ν is equal to $6 \times 10^{12} \text{ cm}^2 \text{ s}^{-1}$ at the top of the domain and decreases with depth as $\bar{\rho}^{-1/2}$, where $\bar{\rho}$ is the mean density varying by a factor of 46 across the domain. The thermal (κ) and magnetic (η) SGS diffusivities have a similar profile, with fixed Prandtl and magnetic Prandtl numbers of $\text{Pr} = \nu/\kappa = 0.25$ and $\text{Pm} = \nu/\eta = 8$ respectively. The large Pm here reflects unresolved turbulent mixing processes, and such a value allows efficient dynamo action with tractable numerical resolution. In the Sun, Pm based on microscopic processes is much smaller, but the relationship between it and the effective turbulent diffusivities is uncertain. At small Pm, the critical magnetic Reynolds number needed for dynamo action increases considerably (Boldyrev & Cattaneo 2004; Schekochihin et al. 2005), rendering simulations much more computationally demanding. The field strengths reported here are likely sensitive to the Pm chosen.

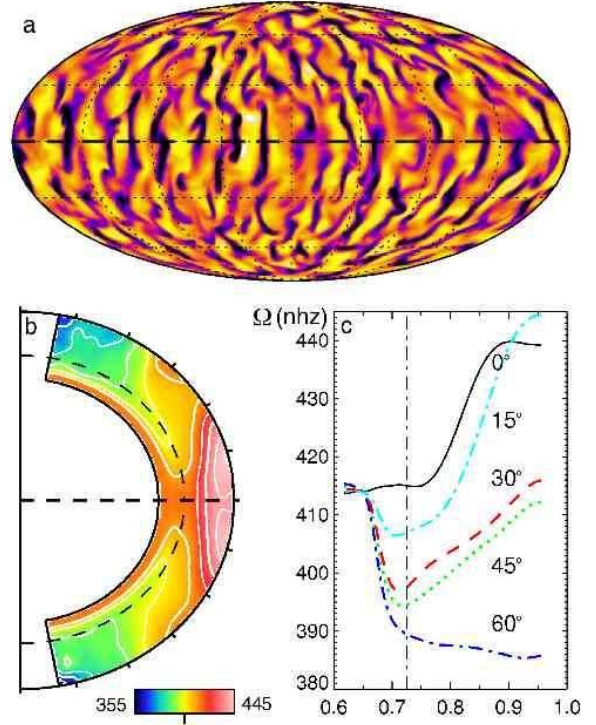


FIG. 1.— (a) Global view (in Mollweide projection) at one instant of radial velocity v_r on a spherical surface at mid-depth ($r = 0.84R$) in the convection zone, with upflows bright and downflows dark. Equator is shown dashed. Angular velocity Ω averaged in time and in longitude, showing (b) contours in radius and latitude and (c) variation with proportional radius along specified latitudinal cuts.

Strong differential rotation is established by the convection. Figure 1b shows the mean angular velocity Ω (relative to the rotating frame) as a contour plot in radius and latitude, and Figure 1c its variation with radius along selected latitudinal cuts. Within the bulk of the convection zone, there is a prominent decrease in Ω from equator to pole. Near the upper boundary, the angular velocity contrast $\Delta\Omega$ (between equator and 60°) is 55 nHz or 13% of the frame rotation rate. In comparison to MBT06 that had no penetrative region, the $\Delta\Omega$ here is reduced and Ω is more constant on cylinders aligned with the rotation axis. Below the base of the convection zone (at $0.73R$) where the stratification is subadiabatic, Ω adjusts rapidly to uniform rotation within a pronounced tachocline of shear. The overall fast equator and slow pole behavior is in keeping with the Ω profiles deduced from helioseismology (e.g., Thompson et al. 2003), but this model possesses more radial shear within the bulk of the convection zone than in the Sun. We have clearly realized a tachocline of strong radial and latitudinal shear, which plays a major role in the organization of large-scale magnetic fields.

Prominent magnetic dynamo action is achieved within this simulation. Much as in BMT04, the seed fields are rapidly amplified, with strong fluctuating magnetic fields ($\sim 3000 \text{ G}$ rms) and weaker mean toroidal and poloidal fields (of time-averaged strengths $\leq 300 \text{ G}$) achieved within the bulk of the convection zone. Over the 2800 simulated days (about 100 rotation periods) studied after the field strengths have largely equilibrated, the dynamo action is persistent, with overall magnetic energy sustained at about 40% of the convective ki-

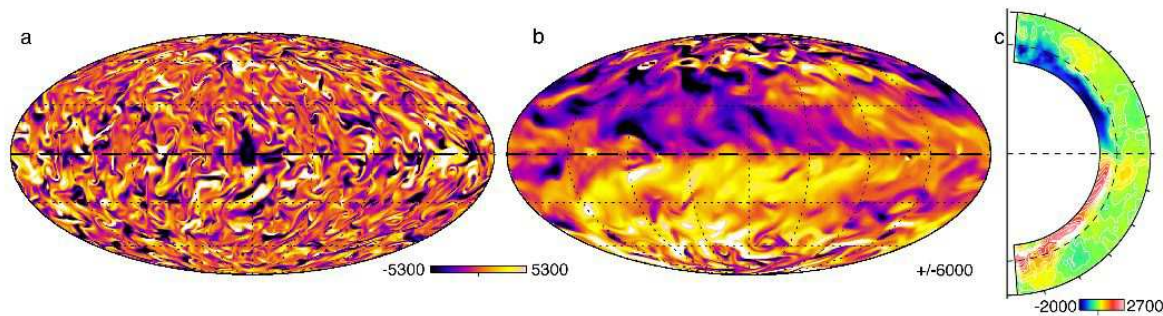


FIG. 2.— Toroidal magnetic fields realized in the convective envelope and underlying radiative region. Mollweide projections at one instant of longitudinal field B_ϕ on a spherical surface (a) at mid-depth in the convection zone ($r = 0.84R$) and (b) in the stable zone ($r = 0.67R$). (c) Contours in radius and latitude of B_ϕ averaged in time (over an interval of 220 days) and in longitude. Field strengths are in G.

netic energy. Figure 2a shows a snapshot of the longitudinal field B_ϕ at mid-depth ($r = 0.84R$), revealing complex structure on many scales, with no evident polarity preferences. The radial and latitudinal fields B_r and B_θ also possess intricate and highly variable structures, tracing the convective flow realized in the bulk of the convection zone. In the underlying stable region (at $r = 0.67R$), Figure 2b shows that the magnetic field has been decidedly organized by the rotational shear, with the longitudinal field there stretched into large toroidal structures that extend around much of the domain. Equally striking is that B_ϕ fields show antisymmetric parity in the stable region, with opposite signs to those in the northern and southern hemispheres. The organized nature of strong toroidal fields in the stable region is confirmed in Figure 2c showing the time-averaged axisymmetric B_ϕ . Here the opposite polarities of the mean toroidal fields are evident in the two hemispheres, as contrasted to the weak and patchy mixed-polarity structures within the convection zone. The time-averaged axisymmetric fields in the stable region attain strengths of order 3000 G, or about ten times stronger than the mean B_ϕ in the convection zone. Whereas fluctuating (non-axisymmetric) fields dominate in the convection zone, the magnetic energy in the mean toroidal field is about three times larger than the fluctuating magnetic energy within the tachocline. The strong toroidal field established in the stable region is accompanied by a largely dipolar poloidal field.

Neither the organization of the magnetic field below the convection zone into predominantly axisymmetric toroidal fields, nor the strong parity selection exhibited here, appear to be transient effects. These attributes arose rather quickly (~ 200 days) after the introduction of the forced tachocline, and have persisted for as long as we have continued the calculations. A sense of the evolution and spatial distribution of the mean fields in our simulation is provided by Figure 3 showing the radial and temporal variations of the axisymmetric toroidal field B_ϕ sampled at latitude -30° . The strongest toroidal fields there are clearly attained in the stable region ($r/R < 0.73$), with some modulations in amplitude but no changes in polarity. Within the convection zone, both the strength and polarity of the weaker toroidal field are more variable. Further investigation reveals that the axisymmetric dipole field both in the convection zone and in the stable region has not changed its overall polarity during the course of our simulation. This is in sharp contrast to the evolution of

the mean dipole component in BMT04, which considered the convection zone in isolation, where the dipole flipped at irregular intervals of less than 600 days. This suggests that the presence of a reservoir of strong toroidal fields with persistent polarity in the stable region is serving to stabilize the mean poloidal field realized in the convection zone.

4. BUILDING STRONG TOROIDAL FIELDS

The predominantly axisymmetric nature of the magnetic fields in the stable region may be understood in two complementary ways. First, the lack of significant non-axisymmetric motions there precludes the generation of strong fluctuating fields like those realized in the convection zone. Thus non-axisymmetric (fluctuating) fields must either diffuse in from the convection zone or be transported downward by overshooting motions. Second, Spruit (1999) has argued that any such fluctuating fields will, in the presence of well-defined angular velocity gradients, be quickly expelled from the system through reconnection between neighboring magnetic surfaces. He estimates that this process acts on a time scale $\tau_\Omega \sim (3r^2\pi^2/\eta\Omega^2q^2)^{1/3}$, with q a measure of the rotational shear. In the Sun, this estimate yields time scales of order 100 years, but in our far more diffusive simulation, τ_Ω is about a year. Thus fluctuating fields pervading the radiative region are fairly quickly erased; they are not replenished from above on a comparable time scale.

The strength of the mean toroidal field below the convection zone is likely strongly influenced by the enhanced diffusive terms and spatially extended tachocline in our simulation. In the kinematic regime, the strength of toroidal fields B_t generated in time t by stretching of poloidal fields B_p due to radial shear is of order $B_t/B_p \sim \Delta v_\phi t / \Delta r$, with Δv_ϕ the radial differential rotation velocity across a length Δr below the convection zone. Thus the strength of the toroidal field depends both on the angular velocity contrast and on how abrupt that contrast is; a narrower tachocline might then yield stronger fields. This estimate suggests that in our simulation, a 10 G poloidal field could be stretched to yield 1 kG toroidal fields in about a year. The magnetic diffusion time scale at the same depth is about 3 years, so fields can be amplified before they are diffused away. The far smaller magnetic diffusion and possibly narrower tachocline in the real solar interior may well lead to even greater amplification of the toroidal field there.

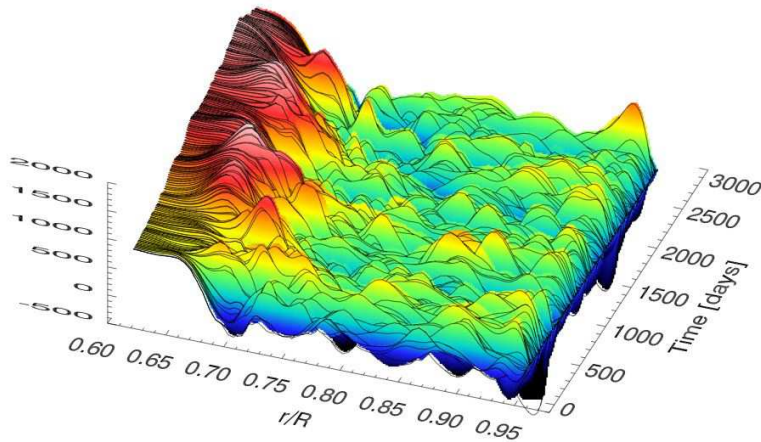


FIG. 3.— Temporal evolution and spatial distribution of axisymmetric toroidal magnetic fields. Variation with radius and time of B_ϕ at a latitude of -30° , with tall peaks (bright tones) corresponding to large positive amplitudes. The strongest fields are realized in the stable region ($r/R < 0.73$), where the polarity of the fields is also remarkably stable over the 2500 days sampled here.

The realization of antisymmetric toroidal field parity within the stable zone is a striking property. It appears to be a robust feature but its origins are currently unclear. The generation of such parity would be expected if a dipolar poloidal field were to be sheared by differential rotation, but no such dipole seeds were introduced. Rather, the initial seed field was toroidal and included both symmetric and antisymmetric components. The emergence of a dipolar mean field may be a consequence

of large-scale self-organization processes such as those associated with the inverse cascade of magnetic helicity in MHD turbulence or the α -effect of mean-field dynamo theory. Such processes may occur within the convection zone where Coriolis forces induce opposite kinetic helicity in the northern and southern hemispheres (as in BMT04). Poloidal fields thus generated may then be pumped into the tachocline where they are stretched into toroidal structures by the shear and amplified. The reservoir of toroidal field thus established within the tachocline may then feed back on field generation in the convection zone, providing the seed for new poloidal field. We plan to assess each of these processes in future work.

In summary, these are the first global three-dimensional MHD simulations of turbulent solar convection to allow penetration into a forced tachocline of rotational shear. We have thus made contact with several of the dynamical processes thought to be essential in the operation of the global solar dynamo. The combined action of convection and an organized tachocline has here yielded magnetic fields that possess several distinctive properties. The significant toroidal fields realized beneath the convection zone, the antisymmetric parity displayed by those fields, and the persistence of a single polarity for multiple years, are reminiscent of the highly organized magnetism that appears as sunspots at the solar surface. Further work to test the robustness of these features has been initiated and will be reported.

This work was partly supported by NASA through Heliophysics Theory Program grant NNG05G124G, and by NSF through an Astronomy and Astrophysics Postdoctoral Fellowship (AST-0502413). The simulations were carried out with NSF PACI support of NCSA, SDSC and PSC, NASA support of Project Columbia, as well as the CEA resource of CCRT and CNRS-IDRIS in France.

REFERENCES

- Boldyrev, S., & Cattaneo, F. 2004, *Phys. Rev. Lett.*, 92, 144501
 Brummell, N. H., Clune, T. L., & Toomre, J. 2002, *ApJ*, 570, 825
 Brun, A. S., Miesch, M. S., & Toomre, J. 2004, *ApJ*, 614, 1073
 Brun, A. S., & Toomre, J. 2002, *ApJ*, 570, 865
 Charbonneau, P. 2005, *Living Rev. Sol. Phys.*, 2, 2, <http://solarphysics.livingreviews.org/lrsp-2005-2/>
 Charbonneau, P., & MacGregor, K. B. 1997, *ApJ*, 486, 502
 Clune, T. L., Elliott, J. R., Glatzmaier, G. A., Miesch, M. S., & Toomre, J. 1999, *Parallel Computing*, 25, 361
 Fan, Y. 2004, *Living Rev. Sol. Phys.*, 1, 1, <http://solarphysics.livingreviews.org/lrsp-2004-1/>
 Gilman, P. A. 1983, *ApJS*, 53, 243
 Glatzmaier, G. A. 1985a, *ApJ*, 291, 300
 Glatzmaier, G. A. 1985b, *Geophys. Astrophys. Fluid Dyn.*, 31, 137
 Miesch, M. S., Elliott, J. R., Toomre, J., Clune, T. L., Glatzmaier, G. A., & Gilman, P. A., 2000, *ApJ*, 532, 593
 Miesch, M. S. 2005, *Living Rev. Sol. Phys.*, 2, 1, <http://solarphysics.livingreviews.org/lrsp-2005-1/>
 Miesch, M. S., Brun, A. S., & Toomre, J. 2006, *ApJ*, 641, 618
 Ossendrijver, M. 2003, *Astron. Astrophys. Rev.*, 11, 287
 Parker, E. N. 1993, *ApJ*, 408, 707
 Schekochihin, A. A., Haugen, N. E. L., Brandenburg, A., Cowley, S. C., Maron, J. L., McWilliams, J. C., 2005, *ApJ*, 625, L115
 Spruit, H. C. 1999, *A&A*, 349, 189
 Thompson, M. J., Christensen-Dalsgaard, J., Miesch, M. S., & Toomre, J. 2003, *ARA&A*, 41, 599